LETTER

doi:10.1038/nature09673

CKIα ablation highlights a critical role for p53 in invasiveness control

Ela Elyada[1]*, Ariel Pribluda[1]*, Robert E. Goldstein[1], Yael Morgenstern[1], Guy Brachya[1], Gady Cojocaru[1], Irit Snir-Alkalay[1], Ido Burstain[1], Rebecca Haffner-Krausz[2], Steffen Jung[3], Zoltan Wiener[4], Kari Alitalo[4], Moshe Oren[5], Eli Pikarsky[1,6] & Yinon Ben-Neriah[1]

The mature gut renews continuously and rapidly throughout adult life, often in a damage-inflicting micro-environment. The major driving force for self-renewal of the intestinal epithelium is the Wnt-mediated signalling pathway, and Wnt signalling is frequently hyperactivated in colorectal cancer[1]. Here we show that casein kinase Iα (CKIα), a component of the β-catenin-destruction complex[1], is a critical regulator of the Wnt signalling pathway. Inducing the ablation of *Csnk1a1* (the gene encoding CKIα) in the gut triggers massive Wnt activation, surprisingly without causing tumorigenesis. CKIα-deficient epithelium shows many of the features of human colorectal tumours in addition to Wnt activation, in particular the induction of the DNA damage response and cellular senescence, both of which are thought to provide a barrier against malignant transformation[2]. The epithelial DNA damage response in mice is accompanied by substantial activation of p53, suggesting that the p53 pathway may counteract the pro-tumorigenic effects of Wnt hyperactivation. Notably, the transition from benign adenomas to invasive colorectal cancer in humans is typically linked to p53 inactivation, underscoring the importance of p53 as a safeguard against malignant progression[3]; however, the mechanism of p53-mediated tumour suppression is unknown. We show that the maintenance of intestinal homeostasis in CKIα-deficient gut requires p53-mediated growth control, because the combined ablation of *Csnk1a1* and either *p53* or its target gene *p21* (also known as *Waf1*, *Cip1*, *Sdi1* and *Cdkn1a*) triggered high-grade dysplasia with extensive proliferation. Unexpectedly, these ablations also induced non-proliferating cells to invade the villous lamina propria rapidly, producing invasive carcinomas throughout the small bowel. Furthermore, in p53-deficient gut, loss of heterozygosity of the gene encoding CKIα caused a highly invasive carcinoma, indicating that CKIα functions as a tumour suppressor when p53 is inactivated. We identified a set of genes (the p53-suppressed invasiveness signature, PSIS) that is activated by the loss of both p53 and CKIα and which probably accounts for the brisk induction of invasiveness. PSIS transcription and tumour invasion were suppressed by p21, independently of cell cycle control. Restraining tissue invasion through suppressing PSIS expression is thus a novel tumour-suppressor function of wild-type p53.

To investigate the physiological roles of CKIα, we generated mice in which *Csnk1a1* was either deleted from the germline or *loxP* flanked (floxed) and therefore able to be conditionally deleted (Supplementary Fig. 1a). Whereas mice that were heterozygous for *Csnk1a1* ($Csnk1a1^{+/-}$) seemed to be normal, homozygous deficiency was embryonic lethal before embryonic day 6.5 (Supplementary Fig. 1b and Supplementary Table 1), suggesting a fundamental role for CKIα in embryogenesis.

To study the role of CKIα in gut physiology, we crossed mice in which *Csnk1a1* was floxed with mice expressing *Vil1*–Cre–ER^{T2}, generating animals in which injection with tamoxifen causes deletion of the gene encoding CKIα exclusively in the intestinal epithelium (hereafter termed $Csnk1a1^{\Delta gut}$ mice). Within 5 days of treatment with tamoxifen, CKIα expression was largely abolished throughout the epithelia of the small bowel (Fig. 1a, b and Supplementary Fig. 2a) and colon (data not shown), and was absent for at least 2 weeks, indicating that intestinal progenitor cells had been targeted by the recombinase Cre. CKIα loss was accompanied by a mild increase in CKIδ expression (Supplementary Fig. 2b), while the priming phosphorylation of β-catenin on the serine residue at position 45 (S45) was abolished, eliminating the rest of the phosphorylation cascade (T41, S37 and S33) (Fig. 1b). Consequently, β-catenin was stabilized in the cytoplasm and nucleus, including in differentiated cells of the villus (Fig. 1a, b and Supplementary Fig. 2d). Using RKO cells (a human colorectal cancer cell line), we confirmed this non-redundant function of the α-isoform of CKI *in vitro* (Supplementary Fig. 2c). These findings indicate that CKIα is indispensable for initiating the β-catenin phosphorylation–degradation cascade in the gut epithelium.

As expected, β-catenin accumulation in the gut of $Csnk1a1^{\Delta gut}$ mice was accompanied by robust activation of many Wnt target genes, including *Myc*, *Axin2*, *Sox9*, *Cd44* and the genes encoding cyclin D1 and cyclin D2 (http://www.stanford.edu/~rnusse/pathways/targets.html) (Fig. 1c, d). Particularly striking was the distinct nuclear expression of cyclin D1, which spread into all villi throughout the small intestine. By contrast, in wild-type small bowel, cyclin D1 was restricted to the crypts. Likewise, CD44 and Myc were overexpressed in $Csnk1a1^{\Delta gut}$ (Fig. 1d). In other mouse models of Wnt hyperactivation, ectopic Paneth cells are common[4], and these are clearly observed in small-bowel villi of $Csnk1a1^{\Delta gut}$ mice (Supplementary Fig. 2e). Thus, knockout of the gene encoding CKIα induced β-catenin stabilization and a massive Wnt response, comparable to other mouse models of Wnt activation and to colorectal cancers.

Surprisingly, despite the robust activation of mitogenic Wnt target genes, gut homeostasis was preserved, and tumorigenesis was not observed. This is in stark contrast to Wnt activation in the mouse gut after deletion of the adenomatosis polyposis coli (*Apc*) gene, which resulted in immediate dysplastic transformation of the entire bowel and rapid death[4]. Instead, we found only mild atypia and minimal small-bowel crypt elongation, owing to an approximately twofold increase in the proliferating cell population (Supplementary Fig. 2e and data not shown). We therefore postulated that *Csnk1a1* ablation elicits a simultaneous reaction that restrains the hyperproliferation and tumorigenesis that is expected on Wnt hyperactivation.

Phenotypic changes in $Csnk1a1^{\Delta gut}$ mice might resemble the oncogene-induced senescence[5] associated with DNA-replication stress, persistent DNA damage[6] and apoptosis[7]. Accordingly, $p19^{ARF}$, a hallmark of oncogene-induced senescence[8], was found to be upregulated

[1]The Lautenberg Center for Immunology, IMRIC, Hebrew University—Hadassah Medical School, Jerusalem 91120, Israel. [2]Department of Veterinary Resources, The Weizmann Institute of Science, Rehovot 76100, Israel. [3]Department of Immunology, The Weizmann Institute of Science, Rehovot 76100, Israel. [4]Molecular Cancer Biology Program and the Institute for Molecular Medicine Finland, Biomedicum Helsinki, University of Helsinki, Helsinki 00014, Finland. [5]Department of Molecular Cell Biology, The Weizmann Institute of Science, Rehovot 76100, Israel. [6]Department of Pathology, IMRIC, Hebrew University—Hadassah Medical School, Jerusalem 91120, Israel.
*These authors contributed equally to this work.

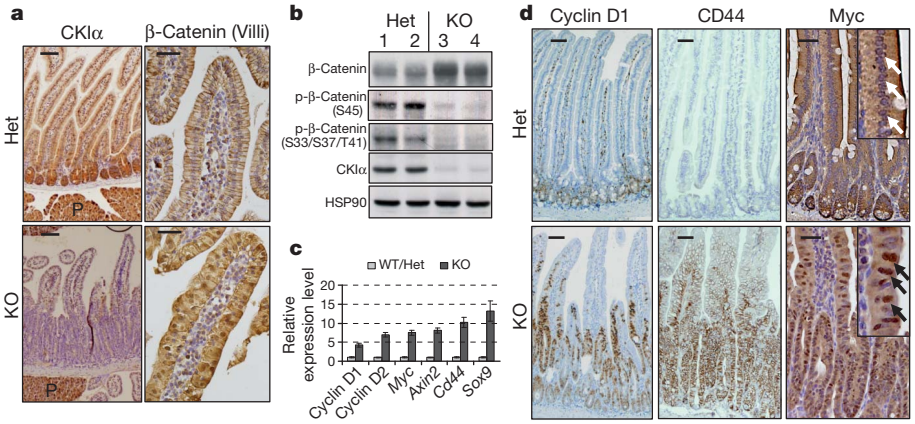

Figure 1 | *Csnk1a1* ablation induces Wnt hyperinduction.
a, Immunohistochemistry analysis of CKIα and β-catenin in heterozygous (*Csnk1a1*$^{+/\Delta gut}$; Het) and homozygous (*Csnk1a1*$^{\Delta gut}$; KO) *Csnk1a1*-deleted mouse gut. For all immunohistochemistry analyses, brown indicates specific immunostaining, and purple indicates nuclear haematoxylin staining. Scale bars, 100 μm (left), 50 μm (right). P, pancreas. **b**, Western blotting analysis of intestinal epithelial cells (IECs) from Het (lanes 1 and 2) and KO (lanes 3 and 4) mice. Numbered lanes represent individual mice. HSP90 is a loading control. p-β-catenin, phospho-β-catenin. **c**, Quantitative real-time PCR (quantitative rtPCR) analysis of Wnt and β-catenin target gene expression in IECs of wild-type (WT) ($n = 3$), Het ($n = 3$) and KO ($n = 6$) mice. Data are presented as mean ± s.e.m. Data for expression by the WT and Het groups were combined and normalized to 1 (denoted WT/Het), and expression by other groups is calculated relative to WT/Het. **d**, Immunohistochemistry analysis of Wnt target gene expression. In the Myc panel, the insets show Myc-negative nuclei in Het cells (white arrows) and Myc-positive nuclei in KO cells (black arrows). Scale bars, 100 μm (left and centre), 50 μm (right).

in *Csnk1a1*$^{\Delta gut}$ enterocytes (Fig. 2c). To assess the potential contribution of cellular senescence in protecting against proliferation and tumorigenesis, we sought signs of persistent DNA damage response (DDR), senescence and apoptosis on *Csnk1a1* ablation in mouse gut, mouse embryonic fibroblasts (MEFs) and primary human fibroblasts. *Csnk1a1* ablation triggered apoptosis, which was evident by TdT-mediated dUTP nick end labelling (TUNEL) assay and cleaved caspase-3 immunostaining (Fig. 2a and Supplementary Fig. 3a), as well as generated widespread signs of DDR (Fig. 2a, 53BP1) and senescence (Fig. 2b). Likewise, ablation of *Csnk1a1* in MEFs and mRNA depletion of the corresponding gene, *CSNK1A1*, in human primary fibroblasts (IMR-90 cells) resulted in a persistent DDR and a senescence phenotype (Supplementary Fig. 3b–f).

The ARF tumour suppressor (p19^{ARF} in mice) and DDR are two major activation arms of the tumour-suppressor protein p53, targeting the two p53 antagonists MDM2 and MDMX (also known as MDM4), respectively[9,10]. Furthermore, *Mdmx* ablation in the gut induced p53 activation and apoptosis, albeit with no tissue abnormalities[11]. *Csnk1a1* ablation in the gut caused marked reduction of MDMX expression (Fig. 2d and Supplementary Fig. 4a). We therefore postulated that the combined effect of p19^{ARF} induction and MDMX degradation might trigger p53 activation in *Csnk1a1*$^{\Delta gut}$ mice. In non-perturbed wild-type gut, p53 is normally inactive[12]. Indeed, p53 expression was undetectable in *Csnk1a1*$^{+/\Delta gut}$ (heterozygous) small or large bowel (Fig. 2d, e and data not shown). By contrast, *Csnk1a1*$^{\Delta gut}$ mice showed marked p53 expression (Fig. 2d, e). Transcriptome analysis revealed that, not only the Wnt cascade, but also the p53 pathway is strongly induced by *Csnk1a1* ablation (Supplementary Table 2; $P = 3.9 \times 10^{-8}$). This was confirmed by monitoring the induction of several specific p53 target genes, including the anti-proliferative gene *p21* (ref. 13) (Fig. 2d, e and Supplementary Fig. 4b). The elevated p53 expression in *Csnk1a1*$^{\Delta gut}$ enterocytes was apparently due to both transcriptional and post-transcriptional control mechanisms; although *p53* (also known as *Trp53*) mRNA was elevated, the fold increase in p53 protein levels exceeded mRNA upregulation (Fig. 2d, e and Supplementary Fig. 7a). Thus, p53 protein stabilization occurred concurrently with β-catenin stabilization in CKIα-depleted RKO (colorectal) cells (Supplementary Fig. 4c). These data point to robust p53 activation in *Csnk1a1*$^{\Delta gut}$ epithelium as a possible means of counteracting the pro-tumorigenic effects of the Wnt pathway.

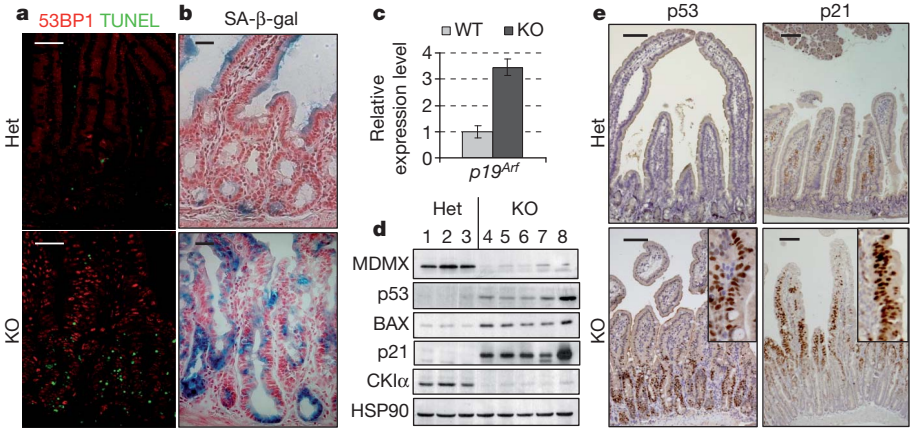

Figure 2 | Persistent DDR and cellular senescence in *Csnk1a1*$^{\Delta gut}$ mice.
a, Double immunofluorescence staining of intestinal sections: TUNEL (an apoptotic marker, green); 53BP1 (a DDR marker, red). Scale bars, 50 μm. **b**, Senescence-associated β-galactosidase (SA-β-gal) staining (blue) and nuclear fast red as a counterstain (pink). Scale bars, 20 μm. **c**, Quantitative rtPCR analysis of IECs of WT ($n = 2$) and KO ($n = 2$) mice. Data are presented as mean ± s.e.m. **d**, Western blotting analysis of IECs from Het (lanes 1–3) and KO (lanes 4–8) mice. HSP90 is a loading control. **e**, Immunohistochemistry analysis of p53 and p21 expression in Het and KO gut. Insets show a threefold magnification of positively stained areas. Scale bars, 100 μm.

As with *Csnk1a1*$^{\Delta gut}$, intestinal *Apc* ablation results in Wnt hyperinduction and widespread cyclin D1 expression[4,14] (Supplementary Fig. 5a). However, the consequences of its ablation—with respect to both homeostasis and tumorigenesis—are profoundly different. One reason for this difference could be p53 activation. We observed only limited, sporadic activation of p53 and its target p21 in intestinal *Apc*$^{\Delta gut}$ epithelium compared with the substantial p53 expression in *Csnk1a1*$^{\Delta gut}$ epithelium (Supplementary Fig. 5a). Supporting these differences were our comparative transcriptome analysis of three enterocyte sources—*Csnk1a1*$^{\Delta gut}$ (Supplementary Table 2), *Apc*$^{\Delta gut}$ (ref. 4) and *Apc*^{1638N} (ref. 15)—showing far greater enrichment of p53 target genes in *Csnk1a1*$^{\Delta gut}$ ($P = 3.9 \times 10^{-8}$) than in the APC-based mouse models ($P = 9.4 \times 10^{-3}$). Differential p53 activation by CKIα depletion was also observed in RKO cells harbouring wild-type *p53* and *Apc* genes. Whereas β-catenin was strongly stabilized when either APC or CKIα was depleted using short hairpin RNAs (shRNAs), H2AX phosphorylation and p53 stabilization were observed only when CKIα was depleted (Supplementary Fig. 5b), indicating that DDR and p53 activation require more than just Wnt activation. Moreover, β-catenin depletion in CKIα-depleted RKO cells did not suppress DDR induction or p53 activation (Supplementary Fig. 5c), demonstrating that CKIα loss induces p53 independently of Wnt hyperinduction. Thus, the absence of intestinal tumours despite Wnt hyperactivation could be due to distinctive activation of p53 when *Csnk1a1* is ablated.

To assess the contribution of p53 to counteracting Wnt-driven tumorigenesis, we crossed *Csnk1a1*$^{\Delta gut}$ mice with *p53*$^{\Delta gut}$ mice. Remarkably, within 2 weeks of initiating the tamoxifen-induced co-ablation, the *Csnk1a1*$^{\Delta gut}$*p53*$^{\Delta gut}$ (double-knockout) mice developed widespread high-grade dysplasia and numerous intramucosal carcinomas invading the lamina propria in most of the small-bowel crypts and villi (Fig. 3a (H&E) and Supplementary Fig. 6a), and they died shortly thereafter. Unlike *Csnk1a1*$^{\Delta gut}$ (knockout) mice, double-knockout mice showed massive proliferation throughout the crypt–villus axis, up to the tips of the villi (Fig. 3a (BrdU) and Supplementary Fig. 6b). This, however, was not attributable to further hyperactivation of Wnt signalling in the double-knockout mice: β-catenin stabilization and Wnt gene induction in double-knockout mice were comparable to those in *Csnk1a1*$^{\Delta gut}$ mice (Supplementary Fig. 6c–f). These data indicate that the tumour-suppressor function of p53 in *Csnk1a1*$^{\Delta gut}$ mice is not exerted through the suppression of Wnt signalling. Whereas the *Bax* induction and activation-associated cleavage of BAX protein seen in *Csnk1a1*$^{\Delta gut}$ mice were absent in double-knockout mice (Supplementary Fig. 7a, b), the extent of apoptosis in double-knockout mice was similar to that in *Csnk1a1*$^{\Delta gut}$ mice (Supplementary Fig. 7c, cleaved caspase 3), indicating that apoptosis by itself, whether p53-dependent or p53-independent, is ineffective at suppressing intestinal carcinogenesis. By contrast, almost no expression of p21 was observed in double-knockout mice (Supplementary Fig. 7b, c), suggesting that p21 might be a key factor in offsetting excessive proliferation and tumorigenesis in *Csnk1a1*$^{\Delta gut}$ mice.

Human colorectal carcinogenesis is a protracted process. It entails multiple genetic mutations and epigenetic events, which propel tumour progression from an aberrant crypt focus through adenoma to invasive carcinoma[3]. In various mouse models, this process, which probably spans 10–15 years in humans, commonly occurs over many months and by a similar sequence of molecular and histological events[16]. The exceptionally rapid development of invasive intramucosal carcinomas in *Csnk1a1*$^{\Delta gut}$*p53*$^{\Delta gut}$ (double-knockout) mice, bypassing the adenomatous phase, prompted us to validate the cancerous nature of the observed lesions. Intestinal villi of double-knockout mice were removed and transplanted under the kidney capsule of immunodeficient (NOD SCID) mice. Invasive adenocarcinomas of intestinal origin permeating the kidney tissue were observed in two of five NOD SCID recipients of double-knockout villi (Fig. 3b), whereas no viable intestinal tissue was detectable in recipients of either CKIα-deficient

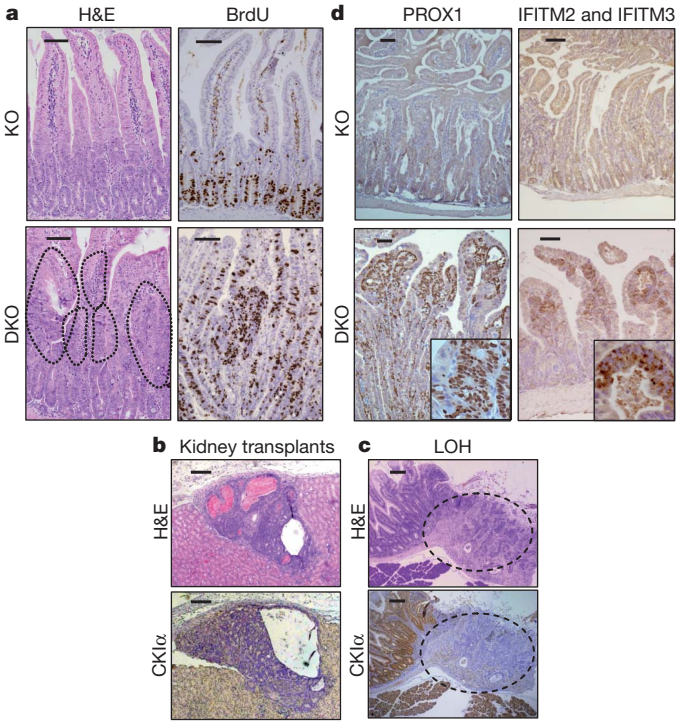

Figure 3 | Widespread invasive carcinomas in the *Csnk1a1*$^{\Delta gut}$*p53*$^{\Delta gut}$ (double-knockout) bowel. **a**, Haematoxylin (nuclear, purple) and eosin (cytoplasmic, pink) (H&E) staining and immunohistochemistry analysis of BrdU (proliferation) in intestinal sections of double-knockout (*Csnk1a1*$^{\Delta gut}$*p53*$^{\Delta gut}$; DKO) mice compared with *Csnk1a1*$^{\Delta gut}$ (KO) mice. Dashed lines in the H&E DKO panel demarcate intramucosal carcinomas. Scale bars, 100 μm. **b**, H&E staining and CKIα immunohistochemistry analysis after transplantation of DKO villi to NOD SCID mice ($n = 2$). CKIα-negative intestinal adenocarcinoma is shown permeating the kidney. Scale bars, 100 μm. **c**, H&E staining and CKIα immunohistochemistry analysis in serial intestinal sections of *Csnk1a1*$^{+/\Delta gut}$*p53*$^{\Delta gut}$ mice (Het mice crossed with *p53* KO mice). Dashed lines demarcate a stage T4 carcinoma. Loss of CKIα protein expression is restricted to the tumour cells. Scale bars, 200 μm. **d**, Immunohistochemistry analysis of PROX1, IFITM2 and IFITM3 expression in KO and DKO gut, as in **a**. Insets show fourfold magnification of intramucosal carcinoma areas. Scale bars, 100 μm.

villi with one functional *p53* allele ($n = 3$) or p53-deficient villi with one functional *Csnk1a1* allele ($n = 2$) (data not shown). This confirmed the occurrence of bona fide carcinogenesis in double-knockout mice.

Further evidence of the potent effect of combined loss of p53 and CKIα came from mice that were heterozygous for the gene encoding CKIα and lacked p53. *Csnk1a1*$^{+/-}$ and *Csnk1a1*$^{-/fl}$ (heterozygous) mice (where fl is a floxed allele) have a full lifespan without evidence of tumorigenesis (data not shown). Likewise, *p53* knockout mice do not develop intestinal tumours, at least until the age of 6 months, by which time they succumb mostly to lymphomas and sarcomas[17]. By contrast, seven of nine mice homozygous for gut-ablated *p53* and harbouring one active *Csnk1a1* allele in the gut (*Csnk1a1*$^{+/\Delta gut}$*p53*$^{\Delta gut}$) developed invasive carcinomas that permeated the bowel muscular wall into the subserosal fat and some of which involved the serosal surface (stage T4) within 6 months of gene ablation. Remarkably, by immunohistochemistry analysis, all of these malignant lesions are CKIα-negative (Fig. 3c). DNA analysis of carcinoma tissue implicated loss of heterozygosity (LOH) at the *Csnk1a1* locus as the source of carcinoma growth (Supplementary Fig. 8). Overall, our data point to a dual role for CKIα: it acts as a tumour suppressor by blocking Wnt-driven proliferation, and its absence activates p53 to counter carcinogenesis.

Whereas p53 inactivation often coincides with the transition of benign colorectal tumour to invasive carcinoma in humans, existing mouse models for colorectal cancer do not clearly show how wild-type p53 suppresses carcinogenesis[18,19]. An advantage of the *Csnk1a1* ablation

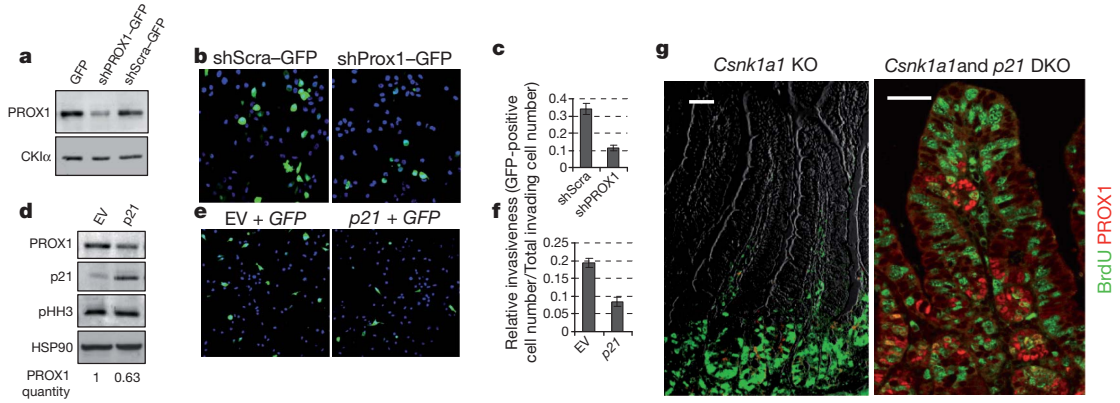

Figure 4 | Invasiveness suppression by p53, through p21. **a**, Western blotting analysis of COLO 205 cells transfected with lentiviral vectors expressing *GFP* and shRNA specific for *PROX1* and *GFP* (shPROX1–GFP), scrambled sequence shRNAs and *GFP* (shScra–GFP) or *GFP* empty vector. CKIα is a loading control. **b**, Matrigel invasion assay of shPROX1–GFP-expressing cells compared with shScra–GFP-expressing cells (GFP, green). Relative transfection efficiencies were 1.07/1. Hoechst stain (blue) was used as a nuclear counterstain, to determine the total number of invading cells. **c**, Quantification (normalized to transfection efficiencies) of Matrigel invasion assay shown in **b**. Data are presented as mean ± s.e.m. **d**, Western blotting analysis of COLO 205 cells transfected with a combination of *p21* and *GFP* expression vectors (*p21* + *GFP*) versus empty vector and *GFP* (EV + *GFP*) (transfection efficiency, 50%). Phospho-histone H3 (pHH3) is a cell cycle marker. HSP90 is a loading control. PROX1 levels were quantified relative to HSP90 and normalized to EV. **e**, Matrigel invasion assay of *p21* and *GFP* co-transfected COLO 205 cells compared with EV and *GFP* co-transfected cells. Relative transfection efficiencies for *p21* and *GFP* versus EV and *GFP* were 1.14/1. Hoechst stain (blue) was used as a nuclear counterstain. **f**, Quantification of data in panel **e**. Data are presented as mean ± s.e.m. **g**, Double immunofluorescence of BrdU (green) and PROX1 (red) in intestinal sections from $Csnk1a1^{\Delta gut}$ (KO) and $Csnk1a1^{\Delta gut}p21^{-/-}$ (DKO) mice. BrdU staining was negative in 83% of cells in invading clusters ($n = 186$) compared with 51% in non-invading epithelia ($n = 354$). Scale bars, 100 μm (left); 50 μm (right).

model is the robust, instantaneous emergence of intramucosal carcinoma, making it easier to track the origin of invasion. To elucidate the molecular basis of invasiveness in $Csnk1a1^{\Delta gut}p53^{\Delta gut}$ mice, we compared the transcriptome of the doubly ablated enterocytes with that of singly ablated ($p53^{\Delta gut}$ or $Csnk1a1^{\Delta gut}$) enterocytes. Among the upregulated genes, there is a subset, which we denote PSIS (p53-suppressed invasiveness signature), associated with diverse invasiveness functions, including loss of enterocyte polarity and adhesion (for example, *Prox1*), tissue remodelling (for example, the *Ifitm* gene family, *Plat* and *Mmp7*) and facilitation of motility (for example, *Pls3*) (Supplementary Table 3 and Supplementary Fig. 9a). *Ifitm* gene family members are new biomarkers for colorectal cancer[20] and are associated with invasion at early stages of human head and neck cancer[21]. PROX1 overexpression characterizes highly dysplastic colorectal adenoma and carcinoma, and it promotes colonic tumorigenesis by modulating polarity and adhesion[22].

We found that *Prox1* and several *Ifitm* gene family members are strongly induced in $Csnk1a1^{\Delta gut}p53^{\Delta gut}$ enterocytes (Supplementary Fig. 9a). These genes harbour TCF-binding sites[23], indicating that they are transcriptionally induced by Wnt signals only if p53-mediated repression is abolished. Immunohistochemistry analysis indicates that PROX1, IFITM2 and IFITM3 proteins are abundantly expressed at foci of $Csnk1a1^{\Delta gut}p53^{\Delta gut}$ intramucosal carcinomas (Fig. 3d), whereas there is little or no expression of these genes in the gut of $Csnk1a1^{+/\Delta gut}$ or $Csnk1a1^{\Delta gut}$ mice. Likewise, expression of PROX1, IFITM2 and IFITM3 is plentiful in the invasive carcinoma that develops following LOH at the *Csnk1a1* locus on a *p53*-null background and after transplantation of double-knockout villi to NOD SCID mice (Supplementary Fig. 9b). Consistent with these findings, the highest expression of PROX1 in human colorectal adenomas is observed in areas of severe dysplasia[22], which are often enriched in p53 mutations[24]. Together, these data point to cells that express PSIS being more capable of invading the lamina propria than neighbouring epithelial cells that do not express PSIS genes.

To confirm direct participation of a PSIS gene in invasiveness control, we depleted PROX1 in COLO 205 cells, a human colorectal cancer cell line in which APC and p53 are mutated. COLO 205 cells show Matrigel invasion on stimulation with phorbol myristate acetate (PMA). Depletion of PROX1 mediated by shRNA (Fig. 4a) resulted in a threefold reduction of Matrigel invasion (Fig. 4b, c). In addition, depletion of p53 in MCF 10A (mammary) cells (which harbour wild-type *p53*) resulted in substantial PROX1 elevation and Matrigel invasion, which was suppressed by co-depletion of p53 and PROX1 (Supplementary Fig. 9c–e). These results indicate that PROX1 expression is a key component of the p53-controlled invasive phenotype.

In addition to its well-known tumour-suppressive role through transcriptional activation of cell cycle inhibitors and pro-apoptotic genes[13], p53 can also mediate transcriptional repression, either through direct association with other transcription factors (for example, NFY[25]) or through the activation of its target gene *p21* (ref. 26). The p21 protein can repress transcription by various mechanisms, including indirect inactivation of E2F transcription factors through the Rb protein pathway, as well as direct binding to E2F1 and Myc[26]. NFY-, E2F- and Myc-binding motifs are abundant among the promoters of genes upregulated in double-knockout mice, and nearly all of the PSIS genes harbour at least one of these binding sites (Supplementary Fig. 10a, b). To examine whether p21 can suppress PSIS and invasiveness, we overexpressed p21 concomitantly with green fluorescent protein (GFP) in COLO 205 cells. The resultant downregulation of PROX1 protein expression (Fig. 4d) and decrease in number of GFP-positive invading cells in a Matrigel assay (Fig. 4e, f) implied PSIS suppression by p21. PROX1 repression by p21 was not due to cell cycle arrest, as p21-overexpressing COLO 205 cells continued to proliferate (Fig. 4d, pHH3). These *in vitro* findings indicated that the p53–p21 pathway may control tissue invasion of epithelial cells through suppression of PSIS-gene expression. Of note, PROX1 expression is insufficient for inducing the invasion phenotype *in vivo*[22]; rather, concerted action of several PSIS genes may be required to promote tissue invasion.

To elucidate the role of p21 in $Csnk1a1^{\Delta gut}$ mice *in vivo*, we generated $Csnk1a1^{\Delta gut}p21^{-/-}$ mice and examined the consequences of dual gene ablation. Much like $Csnk1a1^{\Delta gut}p53^{\Delta gut}$ mice, $Csnk1a1^{\Delta gut}p21^{-/-}$ mice showed Wnt hyperinduction and massive proliferation, as evident from cyclin D1 and 5-bromodeoxyuridine (BrdU) staining spreading into the villi compartment (Supplementary Fig. 11a), indicating that p21 indeed mediates the p53-dependent growth arrest. $Csnk1a1^{\Delta gut}p21^{-/-}$ mice expressed p53 and its typical target genes at $Csnk1a1^{\Delta gut}$-comparable levels (Supplementary Fig. 11b, c); however, like $Csnk1a1^{\Delta gut}p53^{\Delta gut}$ mice, $Csnk1a1^{\Delta gut}p21^{-/-}$ mice developed severe dysplasia and intramucosal carcinomas throughout the small bowel (Supplementary Fig. 11a, H&E), providing direct genetic evidence that p21 is a mediator of

p53-dependent invasiveness control. This was also emphasized by gene expression array analysis showing repression of PSIS genes by p21 (Supplementary Fig. 11d and Supplementary Table 3).

Interestingly, the proliferation rate of the intramucosal carcinoma cells is significantly reduced compared with cells of the adjacent non-invasive epithelium: intramucosal carcinomas upregulate the PSIS marker PROX1 (Fig. 4g and Supplementary Fig. 11a (PROX1)) yet are mostly BrdU-negative (Fig. 4g). Therefore, p21 is a key factor in the suppression of p53-mediated invasiveness, independently of its role in cell cycle control.

Our studies implicate p53 as the guardian of invasiveness. In contrast to a recent report on cell lines[27], we detected no epithelial-to-mesenchymal transition in the $Csnk1a1^{\Delta gut}p53^{\Delta gut}$ bowel (data not shown), distinguishing the invasiveness control function of p53 in intestinal carcinogenesis from other tumour-suppressor mechanisms. Furthermore, there is probably little in common between the invasiveness promotion of a gain-of-function p53 mutant, which functions like an oncogene[28], and the tumour-suppressive property of wild-type p53 described here. For instance, whereas epidermal growth factor receptor signalling is augmented in cells harbouring p53 gain-of-function mutants[28], it does not differ between $Csnk1a1^{\Delta gut}$ and $Csnk1a1^{\Delta gut}p53^{\Delta gut}$ enterocytes (data not shown).

Our $Csnk1a1^{\Delta gut}$ and $Csnk1a1^{\Delta gut}p53^{\Delta gut}$ knockout models recapitulate critical aspects of human colorectal carcinogenesis: Wnt hyperactivation, DDR and senescence, and p53 loss. Whereas Wnt activation, DDR and senescence are early molecular events in human colorectal tumorigenesis, p53 inactivation is typically a late event, concurrent with the transition of benign tumours to invasive colorectal cancer[3]. At this transition point, the control of tissue invasion—rather than the well-established cell-autonomous functions of p53 (apoptosis induction, cell cycle arrest and senescence[7])—is probably the critical tumour-suppressive function of p53. Notably, in the alternative colorectal carcinogenesis model—the '*de novo* colorectal carcinogenesis model'[29], in which, unlike the traditional adenoma–carcinoma sequence[3], invasiveness precedes other aspects of neoplastic growth—p53 loss is an early carcinogenesis event. This alternative model is most common in human colorectal cancer associated with inflammatory bowel diseases[24], possibly indicating that environmental cues, such as inflammatory mediators, may synergize with p53 loss in upregulating PSIS genes, inducing rapid invasiveness. An inflammatory reaction sustaining cellular senescence[30] could fulfil a similar function in the *Csnk1a1* knockout model. We propose that invasion control, which could be triggered early or late in carcinogenesis, is a cardinal tumour-suppressive function of p53 in Wnt-driven tumours.

METHODS SUMMARY

Mice with a genetically modified *Csnk1a1* locus were generated by floxing exons 1 and 2 of the mouse *Csnk1a1* gene. *Pgk1*–Cre mice were used as a full deleter strain, and *Vil1*–Cre–ER^{T2} transgenic mouse as a gut-specific deleter strain. To generate double-knockout mice, $p53^{fl/fl}$ and $p21^{-/-}$ mice were used. Conditional knockouts were induced by subcutaneous or intraperitoneal injection of tamoxifen (Sigma).

Full Methods and any associated references are available in the online version of the paper at www.nature.com/nature.

Received 11 March; accepted 17 November 2010.

1. Clevers, H. Wnt/β-catenin signaling in development and disease. *Cell* **127,** 469–480 (2006).
2. Bartkova, J. *et al.* Oncogene-induced senescence is part of the tumorigenesis barrier imposed by DNA damage checkpoints. *Nature* **444,** 633–637 (2006).
3. Fearon, E. R. & Vogelstein, B. A genetic model for colorectal tumorigenesis. *Cell* **61,** 759–767 (1990).
4. Sansom, O. J. *et al.* Loss of Apc *in vivo* immediately perturbs Wnt signaling, differentiation, and migration. *Genes Dev.* **18,** 1385–1390 (2004).
5. Collado, M. *et al.* Senescence in premalignant tumours. *Nature* **436,** 642 (2005).
6. Di Micco, R. *et al.* Oncogene-induced senescence is a DNA damage response triggered by DNA hyper-replication. *Nature* **444,** 638–642 (2006).
7. Junttila, M. R. & Evan, G. I. p53—a Jack of all trades but master of none. *Nature Rev. Cancer* **9,** 821–829 (2009).
8. Kamijo, T. *et al.* Tumor suppression at the mouse *INK4a* locus mediated by the alternative reading frame product $p19^{ARF}$. *Cell* **91,** 649–659 (1997).
9. Damalas, A., Kahan, S., Shtutman, M., Ben-Ze'ev, A. & Oren, M. Deregulated β-catenin induces a p53- and ARF-dependent growth arrest and cooperates with Ras in transformation. *EMBO J.* **20,** 4912–4922 (2001).
10. Sherr, C. J. Divorcing ARF and p53: an unsettled case. *Nature Rev. Cancer* **6,** 663–673 (2006).
11. Valentin-Vega, Y. A., Box, N., Terzian, T. & Lozano, G. *Mdm4* loss in the intestinal epithelium leads to compartmentalized cell death but no tissue abnormalities. *Differentiation* **77,** 442–449 (2009).
12. Wilson, J. W., Pritchard, D. M., Hickman, J. A. & Potten, C. S. Radiation-induced p53 and $p21^{WAF\text{-}1/CIP1}$ expression in the murine intestinal epithelium: apoptosis and cell cycle arrest. *Am. J. Pathol.* **153,** 899–909 (1998).
13. Riley, T., Sontag, E., Chen, P. & Levine, A. Transcriptional control of human p53-regulated genes. *Nature Rev. Mol. Cell Biol.* **9,** 402–412 (2008).
14. Andreu, P. *et al.* Crypt-restricted proliferation and commitment to the Paneth cell lineage following *Apc* loss in the mouse intestine. *Development* **132,** 1443–1451 (2005).
15. Fodde, R. *et al.* A targeted chain-termination mutation in the mouse *Apc* gene results in multiple intestinal tumors. *Proc. Natl Acad. Sci. USA* **91,** 8969–8973 (1994).
16. Taketo, M. M. & Edelmann, W. Mouse models of colon cancer. *Gastroenterology* **136,** 780–798 (2009).
17. Donehower, L. A. e. t. a. l. Mice deficient for p53 are developmentally normal but susceptible to spontaneous tumours. *Nature* **356,** 215–221 (1992).
18. Fazeli, A. *et al.* Effects of p53 mutations on apoptosis in mouse intestinal and human colonic adenomas. *Proc. Natl Acad. Sci. USA* **94,** 10199–10204 (1997).
19. Reed, K. R. *et al.* A limited role for p53 in modulating the immediate phenotype of *Apc* loss in the intestine. *BMC Cancer* **8,** 162 (2008).
20. Andreu, P. *et al.* Identification of the IFITM family as a new molecular marker in human colorectal tumors. *Cancer Res.* **66,** 1949–1955 (2006).
21. Hatano, H. *et al.* IFN-induced transmembrane protein 1 promotes invasion at early stage of head and neck cancer progression. *Clin. Cancer Res.* **14,** 6097–6105 (2008).
22. Petrova, T. V. *et al.* Transcription factor PROX1 induces colon cancer progression by promoting the transition from benign to highly dysplastic phenotype. *Cancer Cell* **13,** 407–419 (2008).
23. Cole, M. F., Johnstone, S. E., Newman, J. J., Kagey, M. H. & Young, R. A. Tcf3 is an integral component of the core regulatory circuitry of embryonic stem cells. *Genes Dev.* **22,** 746–755 (2008).
24. Yin, J. *et al.* p53 point mutations in dysplastic and cancerous ulcerative colitis lesions. *Gastroenterology* **104,** 1633–1639 (1993).
25. Tabach, Y. *et al.* The promoters of human cell cycle genes integrate signals from two tumor suppressive pathways during cellular transformation. *Mol. Syst. Biol.* **1,** 2005.0022 (2005).
26. Abbas, T. & Dutta, A. p21 in cancer: intricate networks and multiple activities. *Nature Rev. Cancer* **9,** 400–414 (2009).
27. Wang, S. P. *et al.* p53 controls cancer cell invasion by inducing the MDM2-mediated degradation of Slug. *Nature Cell Biol.* **11,** 694–704 (2009).
28. Muller, P. A. *et al.* Mutant p53 drives invasion by promoting integrin recycling. *Cell* **139,** 1327–1341 (2009).
29. Bedenne, L. *et al.* Adenoma–carcinoma sequence or '*de novo*' carcinogenesis? A study of adenomatous remnants in a population-based series of large bowel cancers. *Cancer* **69,** 883–888 (1992).
30. Coppe, J. P., Desprez, P. Y., Krtolica, A. & Campisi, J. The senescence-associated secretory phenotype: the dark side of tumor suppression. *Annu. Rev. Pathol.* **5,** 99–118 (2010).

Supplementary Information is linked to the online version of the paper at www.nature.com/nature.

Acknowledgements We thank S. Robine for the *Vil1*–Cre–ER^{T2} mice, O. Sansom and B. Romagnolo for intestinal sections of $Apc^{\Delta gut}$ mice, K. Rajewsky for the pGEM–*loxP*–Neo–*loxP* and pCA–NLS–Cre vectors; and E. Horwitz, M. Farago, D. Naor, N. Asherie and D. Knigin for providing expertise and reagents. We are grateful to A. Yaron for critical reading of the manuscript. This work was supported by the Dr. Miriam and Sheldon G. Adelson Medical Research Foundation (AMRF), the Israel Science Foundation, the RUBICON EC Network of Excellence, the Israel Cancer Research Fund and Deutsches Krebsforschungszentrum–Ministry of Science and Technology (DKFZ–MOST). Z.W. is supported by a Marie-Curie Intra-European Fellowship.

Author Contributions Most experiments were performed by E.E., A.P. and R.E.G. Additional experimental work was carried out by Y.M., G.B., G.C., I.S.-A., I.B., R.H.-K. and Z.W. Experimental design and interpretation of data were conducted by all authors. S.J. supervised the gene targeting. The project was supervised by E.P. and Y.B.-N., and the paper was written by E.E., A.P., R.E.G., K.A., M.O., E.P. and Y.B.-N.

Author Information Reprints and permissions information is available at www.nature.com/reprints. The authors declare no competing financial interests. Readers are welcome to comment on the online version of this article at www.nature.com/nature. Correspondence and requests for materials should be addressed to Y. B.-N. (yinon@cc.huji.ac.il) and E.P. (peli@hadassah.org.il).

METHODS

Plasmids and embryonic stem cell culture. A CKIα expression vector was constructed on the basis of pGEM-11Zf(+), to which an XbaI- and SalI-digested fragment of a neomycin cassette flanked by two *loxP* sites was inserted from a pL2-neo expression vector. Exons 1 and 2 of the mouse *Csnk1a1* gene were cloned into the vector, flanked by *loxP* sites using a third *loxP* site. Short (1-kilobase) and long (5-kilobase) homology sequences were cloned upstream and downstream of the targeted exons, respectively. All genomic fragments were amplified by PCR from 129/SvJ mouse DNA. The vector was linearized with SalI and purified using phenol–chloroform extraction and ethanol precipitation methods. R1 embryonic stem (ES) cells (129/SvJ-mouse derived) were electroporated and cultured on a feeder layer of MEFs using DMEM supplemented with 15% ES-cell-tested FBS and 1,000 U ml^{-1} ESGRO (Chemicon). Neomycin selection was done in 0.2 mg ml^{-1} G418 (Sigma). pCA–NLS–Cre was used as a Cre expression vector for transient transfection of Cre into ES cells. Selection was done in 2 μg ml^{-1} puromycin.

Aggregation, mouse breeding and genotyping. R1 ES cells were aggregated to CD-1 mouse morulae. Chimaeric mice were bred with CD-1 mice to check for germline transmission. *Pgk1*–Cre transgenic mice[31] were used as a deleter strain for the generation of germline *Csnk1a1* deletion. For generation of conditional *Csnk1a1* knockout mice, Cre was transiently expressed in ES cells to produce specific deletion of the neomycin cassette and an intact floxed *Csnk1a1* allele. A second aggregation was done, and *Vil1*–Cre–ER^{T2} (ref. 32) transgenic mice were used as a gut-specific deleter to generate a conditional *Csnk1a1* knockout mouse. Inducible double-knockout mice (*p53* and *Csnk1a1*) were generated by crossing mice in which *Csnk1a1* was floxed with mice in which *p53* was floxed[33]. $p21^{-/-}$ mice[34] were purchased from the Jackson Laboratory (stock #003263). Double-knockout mice (*p21* and *Csnk1a1*) were generated by crossing mice in which *Csnk1a1* was floxed with $p21^{-/-}$ mice. Mice were kept under specific pathogen-free conditions at The Weizmann Institute of Science and at the Hadassah Medical School of the Hebrew University. All mouse experiments were performed in accordance with guidelines of the relevant institution's ethics committee.

For mouse genotyping, DNA from the tail or ear of 4-week-old pups was extracted by means of standard protocols. For embryo genotyping, a small section of the embryo was taken for DNA preparation. The following primers were used for simultaneous detection of wild-type and null *Csnk1a1* alleles: 5′-AACAAGATGG CGGCCTCG (forward primer for wild-type and null *Csnk1a1*); 5′-CGCACCA GTTTGTATTTTCC (reverse primer for wild-type *Csnk1a1*); and 5′-GGGCGA ATTCTGCAGATATC (reverse primer for null *Csnk1a1*). The following primers were used for simultaneous detection of wild-type and floxed *Csnk1a1* alleles: 5′-CGTGACGCCGACAGAG (forward primer for wild-type *Csnk1a1*); 5′-ATAA GTGGGGGAGGCTGCTA (reverse primer for wild-type *Csnk1a1*); 5′-GCAGG AAGTGGCAGTGAAAC (forward primer for floxed *Csnk1a1*); and 5′-GGGCGA ATTCTGCAGATATC (reverse primer for floxed *Csnk1a1*). Other primers that were used for genotyping: 5′-CACAAAAAACAGGTTAAACCCAG (forward primer for wild-type and floxed *p53*); 5′-AGCACATAGGAGGCAGAGAC (reverse primer for wild-type and floxed *p53*); 5′-AGCAATTCACACGTATTT GG (forward primer for wild-type *p21*); 5′-TGACGAAGTCAAAGTTCCACC (reverse primer for wild-type *p21*); 5′-AAGCCTTGATTCTGATGTGGGC (forward primer for null *p21*); 5′-GCTATCAGGACATAGCGTTGGC (reverse primer for null *p21*); 5′-ATGTCCAATTTACTGACCGTACACC (forward primer for *cre*); and 5′-CGCCTGAAGATATAGAAGATAATCG (reverse primer for *cre*).

Tamoxifen administration, BrdU labelling and tissue preparation. Tamoxifen (Sigma) was dissolved in corn oil (Sigma), and mice were injected either subcutaneously (100 mg kg^{-1} per injection), five to seven injections every other day for 10–14 days, or intraperitoneally (120 mg kg^{-1}) on two consecutive days. At 3–5 days after the last injection, each mouse was injected intraperitoneally with 10 μl g^{-1} BrdU (GE Healthcare) and killed 2 h later. The jejunum, ileum and the entire large intestine were flushed with ice-cold PBS, cut open longitudinally and subjected to fixation in 4% formaldehyde and paraffin embedding (FFPE). Small pieces of jejunum were embedded in Tissue-Tek O.C.T. Compound (Sakura) and frozen at −80 °C. Intestinal epithelial cells (IECs) were isolated from the middle part of the small intestine, as described previously[35] but with slight modifications: intestinal cells were separated into single cells in Hank's balanced salt solution containing 10 mM HEPES, 5 mM EDTA and 0.5 mM dithiothreitol, at 37 °C for 30 min.

Histology, immunohistochemistry, immunofluorescence, *in situ* hybridization and senescence-associated β-galactosidase analysis. Sections (5 μm) were cut for haematoxylin and eosin (H&E) staining and immunohistochemistry analysis. For immunohistochemistry, sections were incubated with antibodies detecting CKIα (C-19; 1/1,000; Santa Cruz Biotechnology), p21 (F-5; 1/50; Santa Cruz Biotechnology), c-Myc (N-262; 1/100; Santa Cruz Biotechnology), PROX1 (1/200; R&D Systems), EPHB2 (1/200; R&D Systems), β-catenin (1/200; BD Transduction), BrdU (Ab3; 1/100; NeoMarkers), cyclin D1 (SP4; 1/125; Lab Vision), CD44 (IM781; 1/200; eBioscience), p53 (CM5; 1/200; Novocastra), cleaved caspase 3 (1/100; Cell Signaling Technology), IFITM2/3-Fragilis (1/400; Abcam) and lysozyme (1/5,000; Dako). Secondary antibodies were horseradish peroxidase (HRP)-polymer anti-mouse, anti-rabbit, anti-goat and anti-rat antibodies (Nichirei, Dako and Biocare). 3,3′-Diaminobenzidine (DAB) chromogen (Lab Vision) was used for detection. For dual detection of apoptosis and DDR, TUNEL (Roche) was performed according to the manufacturer's instructions, followed by overnight incubation with anti-53BP1 antiserum (1/200; Bethyl) and detection with goat anti-rabbit antibodies conjugated to Alexa Fluor 647 (1/1,000; Molecular Probes). For double immunofluorescence of BrdU and PROX1, FFPE slides were blocked with 3% bovine serum albumin (BSA), 5% donkey serum and 0.1% Triton X-100 in Tris-buffered saline with Tween 20 (TBST) for 1 h, incubated for 16 h at 4 °C with primary antibodies as described, and then exposed to donkey anti-mouse antibodies conjugated to Alexa Fluor 488 and donkey anti-goat antibodies conjugated to Alexa Fluor 647 (1/1,000; Molecular Probes). Hoechst stain (1 μg ml^{-1}; Molecular Probes) was used for nuclear counterstaining. For MDMX immunofluorescence, 5 μm sections were cut from O.C.T.-embedded frozen tissues and fixed in cold acetone for 10 min. Sections were blocked and incubated overnight at 4 °C with anti-MDMX antibody (clone 82; 1/500; Sigma) and subjected to goat anti-mouse antibody conjugated to Alexa Fluor 647 (1/1,000; Molecular Probes). *In situ* hybridization with digoxigenin (DIG; Roche)-labelled cryptdin probe[14] was carried out on FFPE sections. Following deparaffinization and rehydration, slides were immersed in 2 M HCl for 15 min, digested with proteinase K (Roche) for 15 min at 37 °C, fixed for 10 min in 4% paraformaldehyde, acetylated with acetic anhydride in 0.1 M triethanolamine solution, pH 8, pre-incubated at 70 °C for 1 h in hybridization buffer (saline sodium citrate (SSC; pH 4.5), 50% formamide, 2% blocking powder (Roche), 5 mmol l^{-1} EDTA, 50 μg ml^{-1} yeast transfer RNA, 0.1% Tween 20, 0.05% 3[3-cholaminopropyl diethylammonio]-1-propane sulphonate and 50 μg ml^{-1} heparin), and incubated with the probe in a humidity chamber for 24–48 h at 70 °C. Following three washes in 2×SSC with 50% formamide, five washes in TBST and blocking for 1 h at 4 °C in TBST containing 0.5% blocking powder (Roche), slides were incubated for 16 h at 4 °C with anti-DIG Fab–alkaline phosphatase (1/2,000; Roche) in blocking solution (Roche). Following five washes in TBST and two rinses in 0.1 M Tris, pH 8.8, containing 0.1 M NaCl, slides were stained with nitroblue tetrazolium/5-bromo-4-chloro-indolyl-phosphate (NBT/BCIP) solution (BM purple; Roche) at 25° C for 1–2 h, dehydrated and mounted. For senescence-associated β-galactosidase (SA-β-gal) staining, 10 μm sections were cut from O.C.T.-embedded frozen tissue and allowed to adhere to coated slides at 25° C for 1 min before fixation for 15 min in PBS containing 0.5% glutaraldehyde (Sigma). Sections were rinsed with PBS, pH 5.5, containing 1 mM $MgCl_2$ and incubated at 37 °C for 16 h in pre-warmed and filtered 5-bromo-4-chloro-3-indolyl-β-D-galactoside (X-gal) solution (0.1% X-gal (Ornat) dissolved in PBS, pH 5.5, containing 1 mM $MgCl_2$, 5 mM potassium ferrocyanide and 5 mM potassium ferricyanide). Sections were rinsed with PBS, post-fixed in 95% ethanol, rehydrated, counterstained with nuclear fast red, dehydrated and mounted.

Western blotting and RNA analysis. Protein was extracted by whole-cell-extract protocols from cell pellets in protein lysis buffer containing protease and phosphatase inhibitors (*p*-nitrophenyl phosphate (PNPP), sodium orthovanadate (Na_3VO_4), leupeptin, aprotinin, β-glycerophosphate and okadaic acid). Western blotting analysis was performed by means of standard techniques. Blots were incubated with antibodies detecting β-catenin (1/2,500; BD Transduction), phospho-β-catenin (S45; 1/750; Cell Signaling Technology), phospho-β-catenin (S33/S37/T41; 1/750, Cell Signaling Technology), phospho-β-catenin (T41/S45; 1/750; Cell Signaling Technology), CKIα (C-19; 1/1,000; Santa Cruz Biotechnology), CKIε (1/250; Santa Cruz Biotechnology), CKIδ (1/4000; Icos), HSP90α (1/5,000; Calbiochem), tubulin (1/5,000; Sigma), MDMX (clone 82; 1/1,000; Sigma), mouse p53 (CM5; 1/1,000; Novocastra), BAX (1/200; Santa Cruz Biotechnology), p21 (F-5; 1/200; Santa Cruz Biotechnology), MKP1 (1/750; Santa Cruz), $p19^{ARF}$ (1/100; Upstate), human p53 (DO-1/1801 hybridoma mix; 1/10), phospho-Jun (S63; 1/1,000; Cell Signaling Technology), phospho-histone H2A.X (S139; 1/1,000; Millipore), PP2A-C (1/1,000; rabbit serum provided by D. Virshup), cyclin D1 (SP4; 1/500; Lab Vision) and PROX1 (1/1,000; R&D Systems). Secondary antibodies were HRP-linked goat anti-mouse, goat anti-rabbit, goat anti-rat and rabbit anti-goat antibodies (all 1/10,000; Jackson). Blots were developed using ECL (GE Healthcare). Total RNA was extracted from cell pellets using TRI Reagent (Sigma) and phenol–chloroform methods. RNA (2 μg) was subjected to reverse transcription using M-MLV RT (Invitrogen), and mRNA expression levels were measured by quantitative real-time PCR using SYBR Green (Invitrogen) in a 7900HT Fast Real-Time PCR system (ABI). Relative quantities of gene transcripts were analysed in qBase 1.3.5 software and normalized to the *Ubc* and *Hprt* transcripts. Sequences of PCR primers are as follows: 5′-TAGGCGGAATGAAGATGG AC (forward primer for *Axin2*); 5′-CTGGTCACCCAACAAGGAGT (reverse primer for *Axin2*); 5′-ATGCGTCCACCAAGAAGCTGA (forward primer for *Bax*); 5′-AGCAATCATCCTCTGCAGCTCC (reverse primer for *Bax*); 5′-CAGTATC TCCCGGACTGAGG (forward primer for *Cd44*); 5′-GCCAACTTCATTTGGTC

CAT (reverse primer for *Cd44*); 5′-GGTGCGGAAGATCGGATCT (forward primer for *Csnk1a1*); 5′-TTCACTGCCACTTCCTCGC (reverse primer for *Csnk1a1*); 5′-TGAGCCCCTAGTGCTGCAT (forward primer for *Myc*); 5′-AGCCCGAC TCCGACCTCTT (reverse primer for *Myc*); 5′-TTGACTGCCGAGAAGTTGTG (forward primer for cyclin D1); 5′-CCACTTGAGCTTGTTCACCA (reverse primer for cyclin D1); 5′-CACCGACAACTCTGTGAAGC (forward primer for cyclin D2); 5′-TGCTCAATGAAGTCGTGAGG (reverse primer for cyclin D2); 5′-GCT GGCGCTATCTATCCTTG (forward primer for cyclin G1); 5′-GGTCAAATCTC GGCCACTTA (reverse primer for cyclin G1); 5′-GTTAAGCAGTACAGCC CCAAA (forward primer for *Hprt*); 5′- AGGGCATATCCAACAACAAACTT (reverse primer for *Hprt*); 5′-ATCTCCACGCCTGACCATGT (forward primer for *Ifitm1*); 5′-CACCCACCATCTTCCTGTCC (reverse primer for *Ifitm1*); 5′-CTG CTGCCTGGGCTTCATAG (forward primer for *Ifitm3*); 5′-GGATGCTGAGG ACCAAGGTG (reverse primer for *Ifitm3*); 5′-TACCTGCCCCTACCCTGATG (forward primer for *Ly6a*); 5′-AGGAGGGCAGATGGGTAAGC (reverse primer for *Ly6a*); 5′-TGTGTGAGCTGAGGGAGATG (forward primer for *Mdm2*); 5′-CA CTTACGCCATCGTCAAGA (reverse primer for *Mdm2*); 5′-TCACTAATGCCA AACAGTCCAA (forward primer for *Mmp7*); 5′-AAGGCATGACCTAGAGTG TTCC (reverse primer for *Mmp7*); 5′-GTCACACGACTGGGCGATT (forward primer for $p19^{Arf}$); 5′-GACTCCATGCTGCTCCAGAT (reverse primer for $p19^{Arf}$); 5′-TCCACAGCGATATCCAGACA (forward primer for *p21*); 5′-AGACAACGGC ACACTTTGCT (reverse primer for *p21*); 5′-TGAAACGCCGACCTATCCTTA (forward primer for *p53*); 5′-GGCACAAACACGAACCTCAAA (reverse primer for *p53*); 5′-TGGAGAGGGTCAGAAAGCAAA (forward primer for *Pls3*); 5′-AA TCCACAACCGCCAAACTG (reverse primer for *Pls3*); 5′-AGTTCCTGCTGG GTGCTGTC (forward primer for *Plat*); 5′-CGGGGACCACCCTGTATGTT (reverse primer for *Plat*); 5′-ATACCGAGCCCTCAACATGC (forward primer for *Prox1*); 5′-CGTAACGTGATCTGCGCAAC (reverse primer for *Prox1*); 5′-CAAG AAGAGCAGCATCGACA (forward primer for *Puma*); 5′-TAGTTGGGCTCCA TTTCTGG (reverse primer for *Puma*); 5′-GGAGCTCAGCAAGACTCTGG (forward primer for *Sox9*); 5′-TGTAATCGGGGTGGTCTTTCT (reverse primer for *Sox9*); 5′-CAGCCGTATATCTTCCCAGACT (forward primer for *Ubc*); 5′-CTC AGAGGGATGCCAGTAATCTA (reverse primer for *Ubc*).

Villi transplantation and LOH analyses. $Csnk1a1^{\Delta gut}p53^{\Delta gut}$ (double-knockout) male mice ($n = 2$) were used as donors of intestinal villi, with $Csnk1a1^{\Delta gut}p53^{+/\Delta gut}$ ($n = 2$) and $Csnk1a1^{+/\Delta gut}p53^{\Delta gut}$ ($n = 2$) mice as controls. After knockout induction for 12 days and concomitant treatment for 1 week with an antibiotic mix of imipenem, vancomycin and metronidazole (each 0.25 mg ml^{-1}) in the drinking water, the mice were killed, their small intestines flushed twice with PBS and inverted, and their villi scraped from the upper mucosal layer. Villi were centrifuged and resuspended in 1 ml PBS. NOD SCID male mice aged 8 weeks were used as recipients for intestinal villi. The recipient mice were anaesthetized with ketamine/xylazine, the left kidney was exposed, and 200 µl resuspended villi from donors were transplanted under the kidney capsule[36]. Five mice received double-knockout villi, three received $Csnk1a1^{\Delta gut}p53^{+/\Delta gut}$ villi and two received $Csnk1a1^{+/\Delta gut}p53^{\Delta gut}$ villi. Transplanted recipient mice were kept in specific-pathogen-free conditions and given the above antibiotic mix in their drinking water. Six weeks after transplantation, the recipients were killed and FFPE sections of the kidneys were analysed. For LOH analysis, laser capture microdissection was carried out to obtain DNA from normal and cancerous tissues, extracted by means of standard protocols. PCR was performed with the following primers: 5′-GTAATTGGACCCGATGAATCG (forward primer), 5′-AAACGCAGCAGTGCAACAAAC (reverse primer), detecting 126 base pairs (bp) and 187 bp wild-type and floxed *Csnk1a1* alleles, respectively; 5′-CTAGCTTGGCTGGACGTAAAC (forward primer), 5′-AAACGCAGCAGT GCAACAAAC (reverse primer), detecting 150 bp of *Csnk1a1* null allele.

Cell cultures and shRNA depletions. Human fibroblasts (IMR-90) at early passage were grown with MEM supplemented with 10% serum. Cells were split after 2 days and left in culture for a total of 8 days, then split again and analysed at sub-confluence for SA-β-gal and γ-H2AX nuclear foci, after a total of 10 days in culture. $Csnk1a1^{+/+}$, $Csnk1a1^{+/fl}$ and $Csnk1a1^{fl/fl}$ MEFs were collected from embryonic day 13.5 mice and prepared according to standard procedures. Early-passage MEFs were seeded at 1×10^6 cells per 10-cm dish and grown with DMEM supplemented with 10% serum. The floxed *Csnk1a1* allele was subjected to Cre-mediated excision by transduction of the cells with 5×10^7 plaque-forming units (PFU) ml^{-1} of Cre-expressing adenovirus (Ad-Cre) (Gene Transfer Vector Core, University of Iowa). Cells were collected 6 days after transduction with Ad-Cre. Cells ($n \geq 100$) were counted by a cytometer, and their duplication rates were calculated. RKO cells were grown in DMEM supplemented with 10% serum. MG132 (20 µM; Calbiochem) was added for 3 h before cell collection. For cycloheximide treatment, RKO cells were transduced with shRNA vector for 7 days, then treated with 2 µg ml^{-1} doxorubicin for 3 h or left untreated. Cells were then washed, incubated with 40 µg ml^{-1} cycloheximide for the indicated times, and collected. COLO 205 human colorectal cells were grown in RPMI supplemented with 10% serum. Transfection into COLO 205 cells was done using Amaxa Cell Line Nucleofector Kit T (Lonza), and cells were collected 48 h after transfection. MCF 10A breast epithelial cells were grown in F12/DMEM. SA-β-gal staining for human and mouse fibroblasts was carried out as described previously[37]. Cells were then washed with PBS, fixed in 4% paraformaldehyde for 15 min, washed with TBS, incubated for 10 min in 0.25% Triton X-100-containing TBS, washed with TBS, blocked in 3% BSA with 0.1% Triton X-100/TBS for 1 h and incubated for 16 h with anti-phospho-histone H2A.X (S139) antibody (1/1,000; Upstate). Staining was detected as described above. As a positive control for senescence and DDR, cells were treated with 30 Gy ionizing irradiation. pLKO-based (Open Biosystems) and pLL3.7-based lentiviral vectors were used to transduce cells with shRNA-encoding sequences. The lentiviral packaging system was provided by I. Verma[38,39]. Human shRNA-encoding sequences that were used are as follows: *CSNK1A1* 5′-GCAGAAT TTGCGATGTACTTA; *CSNK1D* and *CSNK1E* 5′-GGGCTTCTCCTATGACTAC; *APC* 5′-GCAGAGGAAGGTGATATTC; β-catenin 5′-GTGGGTGGTATAGAGG CTC; $p19^{Arf}$ 5′-GTGATGATGATGGGCAACGTT; scrambled control 5′-TCCTA AGGTTAAGTCGCCCTCG; *p53* 5′-CGGCGCACAGAGGAAGAGAAT; *PROX1* 5′-TGAGCCAGTTTGATATGGATTTCAAGAGAATCCATATCAAACTGGCT CTTTTTTC; scrambled control 5′-TGGTCGAACGTCTACTGGAATTCAAGAG ATTCCAGTAGACGTTCGACCTTTTTTC. Mouse shRNA-encoding sequence that was used: mSAF (encoded by *Hnrnpu*) 5′-CTGATGAAGTTGAACTCTC. A combination of CMV–p21 and CMV–GFP expression vectors was used for over-expression of p21, at a ratio of 10/1, respectively. CMV empty vector was used as a control.

Matrigel invasion assay. The *in vitro* Matrigel invasion assay was carried out in 8 µm Transwell dishes. Matrigel (BD Biosciences) was added to each well (20 µg per well) and was left to gel for at least 1 h. MCF 10A cells were seeded at low and high densities on top of the Matrigel and incubated for 20 h at 37 °C. For visualization, invasive cells were fixed in 4% paraformaldehyde and stained with 0.3% crystal violet. COLO 205 cells were seeded on top of the Matrigel and incubated for 48 h at 37 °C. To induce invasion of COLO 205 cells, 12.5 ng ml^{-1} PMA[40] was added to the lower chambers. For visualization, invasive cells were fixed in 4% paraformaldehyde and stained with Hoechst stain.

cDNA array and transcription factor analyses. Gene expression was compared between $Csnk1a1^{+/+}$ (WT), $Csnk1a1^{+/\Delta gut}$ (Het) and $Csnk1a1^{\Delta gut}$ (KO) using Mouse Genome 430 2.0 Arrays (Affymetrix). Gene expression was compared between $Csnk1a1^{+/\Delta gut}$ (Het), $Csnk1a1^{\Delta gut}$ (KO), $Csnk1a1^{+/\Delta gut}p53^{\Delta gut}$ (*p53* KO) and $Csnk1a1^{\Delta gut}p53^{\Delta gut}$ (*Csnk1a1* and p53 DKO) using Mouse Gene 1.0 ST Arrays (Affymetrix). Gene Expression Omnibus accession number for microarray data is GSE24760. RNA was purified from two biological replicates in each group using the TRIzol extraction method (Invitrogen). Labelled cRNA was produced and hybridized according to manufacturer's instructions at the Center for Genomic Technologies, Hebrew University. Gene intensities were extracted from CEL files with Expression Console 1.1 (Affymetrix), using the RMA-Sketch method. Raw data were normalized using median intensities[41]. For each pair of biological replicates, the geometric mean and the ratio were calculated. Transcription factor occurrence was calculated using the DiRE program[42]. Cutoff was defined as the 20 genes with the highest importance score.

31. Lallemand, Y., Luria, V., Haffner-Krausz, R. & Lonai, P. Maternally expressed PGK-Cre transgene as a tool for early and uniform activation of the Cre site-specific recombinase. *Transgenic Res.* **7,** 105–112 (1998).
32. el Marjou, F. *et al.* Tissue-specific and inducible Cre-mediated recombination in the gut epithelium. *Genesis* **39,** 186–193 (2004).
33. Jonkers, J. *et al.* Synergistic tumor suppressor activity of BRCA2 and p53 in a conditional mouse model for breast cancer. *Nature Genet.* **29,** 418–425 (2001).
34. Brugarolas, J. *et al.* Radiation-induced cell cycle arrest compromised by p21 deficiency. *Nature* **377,** 552–557 (1995).
35. Greten, F. R. *et al.* IKKβ links inflammation and tumorigenesis in a mouse model of colitis-associated cancer. *Cell* **118,** 285–296 (2004).
36. Davalli, A. M. *et al.* A selective decrease in the β cell mass of human islets transplanted into diabetic nude mice. *Transplantation* **59,** 817–820 (1995).
37. Dimri, G. P. & Campisi, J. Molecular and cell biology of replicative senescence. *Cold Spring Harb. Symp. Quant. Biol.* **59,** 67–73 (1994).
38. Naldini, L., Blomer, U., Gage, F. H., Trono, D. & Verma, I. M. Efficient transfer, integration, and sustained long-term expression of the transgene in adult rat brains injected with a lentiviral vector. *Proc. Natl Acad. Sci. USA* **93,** 11382–11388 (1996).
39. Naldini, L. *et al. In vivo* gene delivery and stable transduction of nondividing cells by a lentiviral vector. *Science* **272,** 263–267 (1996).
40. Ko, C. H., Shen, S. C., Lee, T. J. & Chen, Y. C. Myricetin inhibits matrix metalloproteinase 2 protein expression and enzyme activity in colorectal carcinoma cells. *Mol. Cancer Ther.* **4,** 281–290 (2005).
41. Irizarry, R. A. *et al.* Exploration, normalization, and summaries of high density oligonucleotide array probe level data. *Biostatistics* **4,** 249–264 (2003).
42. Gotea, V. & Ovcharenko, I. DiRE: identifying distant regulatory elements of co-expressed genes. *Nucleic Acids Res.* **36,** W133–W139 (2008).